ORGANIC LETTERS

2011
Vol. 13, No. 22
6026–6029

Anthracene-Fused BODIPYs as Near-Infrared Dyes with High Photostability

Lintao Zeng,[†] Chongjun Jiao,[†] Xiaobo Huang,[†] Kuo-Wei Huang,[‡] Wee-Shong Chin,[†] and Jishan Wu*,[†]

Department of Chemistry, National University of Singapore, 3 Science Drive 3, 117543 Singapore, and KAUST Catalysis Center and Division of Chemical and Life Sciences and Engineering, King Abdullah University of Science and Technology, 4700 King Abdullah University of Science and Technology, Thuwal 23955-6900, Kingdom of Saudi Arabia

chmwuj@nus.edu.sg

Received September 14, 2011

ABSTRACT

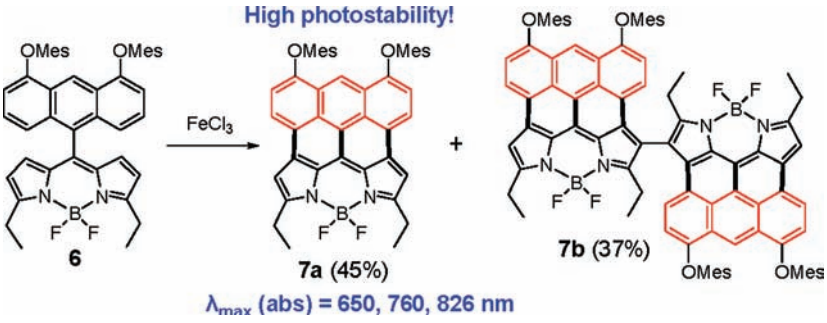

An anthracene unit was successfully fused to the zigzag edge of a boron dipyrromethene (BODIPY) core by an $FeCl_3$-mediated oxidative cyclodehydrogenation reaction. Meanwhile, a dimer was also formed by both intramolecular cyclization and intermolecular coupling. The anthracene-fused BODIPY monomer 7a and dimer 7b showed small energy gaps (~1.4 eV) and near-infrared absorption/emission. Moreover, they exhibited high photostability.

Organic near-infrared (NIR) dyes[1] which function (absorption and/or emission) in the NIR spectral region ranging from 700 to 2000 nm have attracted great attention because of their diverse applications for high-contrast bioimaging,[2] optical recording,[3] NIR laser filter,[4] NIR photography,[5] and solar cells.[6] For instance, for practical applications such as solar cells, the materials should have good light harvesting capability not only at the UV−vis spectral range but also at the NIR range given that sunlight possesses 50% of its radiation energy in the infrared region. In addition, NIR fluorescent dyes have obvious advantages over traditional visible fluorescent probes such as deeper light penetration, low light scattering, and low background interference, which make them widely used in bioimaging and biolabeling.[7] However, many of the reported NIR dyes (e.g., cyanine or polyene dyes) showed poor photostability and chemical stability. Therefore, it is highly desired to develop new NIR dyes with high photostability.

[†] National University of Singapore.
[‡] King Abdullah University of Science and Technology.

(1) For reviews in NIR dyes, see: (a) Fabian, J.; Nakanzumi, H.; Matsuoka, M. *Chem. Rev.* **1992**, *92*, 1197. (b) Qian, G.; Wang, Z. *Chem. Asian J.* **2010**, *5*, 1006. (c) Jiao, C.; Wu, J. *Curr. Org. Chem.* **2010**, *14*, 2145. (d) Sun, Z.; Wu, J. *Aust. J. Chem.* **2011**, *64*, 519.

(2) (a) Kiyose, K.; Kojima, H.; Nagano, T. *Chem. Asian J.* **2008**, *3*, 506. (b) Amiot, C. L.; Xu, S. P.; Liang, S.; Pan, L. Y.; Zhao, X. J. *Sensors* **2008**, *8*, 3082.

(3) Emmelius, M.; Pawlowski, G.; Vollmann, H. W. *Angew. Chem., Int. Ed.* **1989**, *28*, 1445.

(4) Kololuoma, T.; Oksanen, J. A. I.; Raerinne, P.; Rantala, J. T. *J. Mater. Res.* **2001**, *16*, 2186.

(5) Tani, T.; Kikuchi, S. *Photogr. Sci. Eng.* **1967**, *11*, 129.

(6) (a) Imahori, H.; Umeyama, T.; Ito, S. *Acc. Chem. Res.* **2009**, *42*, 1809. (b) Yum, J. H.; Baranoff, E.; Wenger, S.; Nazeeruddin, M. K.; Grätzel, M. *Energy Environ. Sci.* **2011**, *4*, 842. (c) Jiao, C.; Zu, N. N.; Huang, K.; Wang, P.; Wu, J. *Org. Lett.* **2011**, *13*, 3652.

(7) (a) West, J. L.; Halas, N. J. *Annu. Rev. Biomed. Eng.* **2003**, *5*, 285. (b) Ntziachristos, V.; Ripoll, J.; Wang, L. V.; Weissleder, R. *Nat. Biotechnol.* **2005**, *23*, 313. (c) Wang, M.; Mi, C.-C.; Wang, W. X.; Liu, C.-H.; Wu, Y.-F.; Xu, Z.-R.; Mao, C. B.; Xu, S.-K. *ACS Nano* **2009**, *3*, 1580. (d) Murtagh, J.; Frimannsson, D. O.; O'Shea, D. F. *Org. Lett.* **2009**, *11*, 5386. (e) Tasior, M.; O'Shea, D. F. *Bioconjugate Chem.* **2010**, *21*, 1130.

10.1021/ol202493c
Published on Web 10/20/2011

4,4-Difluoro-4-bora-3a,4a-diaza-*s*-indacene, also known as boron dipyrromethene (BODIPY), is a class of highly fluorescent organic fluorophore.[8] Its extraordinary chemical and physical properties, such as high quantum yield, large extinction coefficient, and good thermal and photochemical stability, make it attractive for wide applications including luminescent devices,[9] biological imaging and labeling,[10] sensors,[11] and dye-sensitized solar cells (DSCs).[12] The BODIPY core usually exhibits visible absorption and emission located between 470 to 550 nm. To further push the absorption/emission wavelength to far-red and even the NIR region, a variety of strategies have been used: (1) extension of π-conjugation by fusing rigid ring to the pyrrole unit (e.g., replacing pyrrole with isoindole),[13] (2) functionalization at the α- and/or *meso*-position to generate a "push−pull" motif,[14] and (3) replacement of the 8-carbon atom with a nitrogen atom to form aza-BODIPY dyes.[15] Very recently, our group developed a new strategy by fusing an aromatic unit to the zigzag edge of a BODIPY core via intramolecular oxidative cyclodehydrogenation reaction.[16] By this approach, perylene- and porphyrin-fused BODIPY NIR dyes with long-wavelength absorption/emission and high photostability have been successfully prepared. The major challenge is the choice of an aromatic unit with appropriate geometric and electronic structure, both of which play important role on the cyclodehydrogenation reaction. Anthracene, an electron-rich aromatic hydrocarbon with zigzag edges that potentially match the zigzag edge of a BODIPY core, is therefore tested in this work with the objective of obtaining new anthracene-fused BODIPY NIR dyes.

Scheme 1. Synthetic Route for Compounds **7a** and **7b**

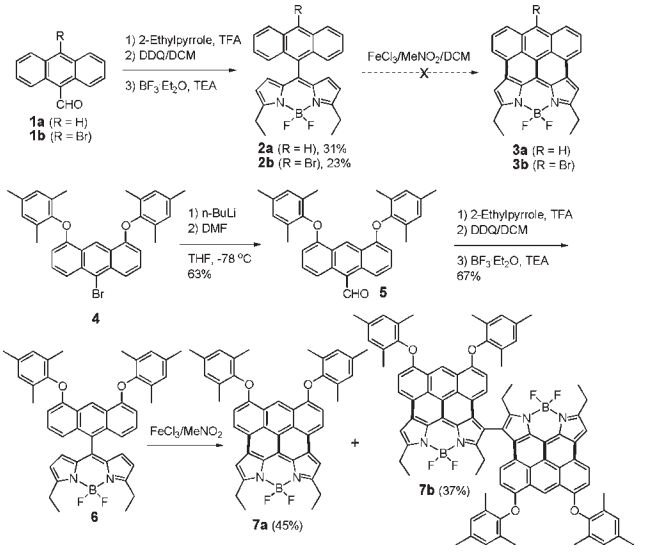

As shown in Scheme 1, three anthracene-BODIPY dyads **2a**, **2b**, and **6** were first prepared and then submitted to an $FeCl_3$-mediated oxidative cyclodehydrogenation reaction to generate fused π-systems. The anthracene monoaldehyde **1a** (R = H)[17] and **1b** (R = Br)[18] condensed with 2-ethylpyrrole in the presence of trifluoroacetic acid (TFA) followed by oxidative dehydrogenation with 2,3-dichloro-5,6-dicyano-1,4-benzoquinone (DDQ) and complexation with $BF_3 \cdot Et_2O$ to give the corresponding anthracene–BODIPY dyads **2a** and **2b** in 31% and 23% yield, respectively. However, treatment of **2a** or **2b** with excessive anhydrous $FeCl_3$ in nitromethane and dichloromethane (DCM) did not afford the target products **3a** or **3b**. Alternatively, inseparable BODIPY oligomers via intermolecular coupling together with other decomposed BODIPY side products were obtained. This failure may be ascribed to the relatively low reactivity at the 1,8-positions of the anthracene unit in **1a** and **1b**. A similar problem was also observed during the synthesis of anthracene-fused porphyrins.[19] To resolve this problem, two strongly

(8) (a) Loudet, A.; Burgess, K. *Chem. Rev.* **2007**, *107*, 4891. (b) Ziessel, R.; Ulrich, G.; Harriman, A. *New J. Chem.* **2007**, *31*, 496. (c) Ulrich, G.; Ziessel, R.; Harriman, A. *Angew. Chem., Int. Ed.* **2008**, *47*, 1184.

(9) (a) Lai, R. Y.; Bard, A. J. *J. Phys. Chem. B* **2003**, *107*, 5036. (b) Hepp, A.; Ulrich, G.; Schmechel, R.; von Seggern, H.; Ziessel, R. *Synth. Met.* **2004**, *146*, 11. (c) Bonardi, L. K.; Camerel, F.; Jolinat, P.; Retailleau, P.; Ziessel, R. *Adv. Funct. Mater.* **2008**, *18*, 401.

(10) (a) Knaus, H.-G.; Moshammer, T.; Friedrich, K.; Kang, H. C.; Haughland, R. P.; Glossmann, H. *Proc. Natl. Acad. Sci. U.S.A.* **1992**, *89*, 3586. (b) Merino, E. J.; Weeks, K. M. *J. Am. Chem. Soc.* **2005**, *127*, 12766. (c) Meng, Q.; Kim, D. H.; Bai, X.; Bi, L.; Turro, N. J.; Ju, J. *J. Org. Chem.* **2006**, *71*, 3248. (d) Peters, C.; Billich, A.; Ghobrial, M.; Hoegenauer, K.; Ullrich, T.; Nussbaumer, P. *J. Org. Chem.* **2007**, *72*, 1842–1845. (e) Li, Z.; Bittman, R. *J. Org. Chem.* **2007**, *72*, 8376.

(11) (a) Yamada, K.; Nomura, Y.; Citterio, D.; Iwasawa, N.; Suzuki, K. *J. Am. Chem. Soc.* **2005**, *127*, 6956. (b) Wang, J.; Qian, X. *Org. Lett.* **2006**, *8*, 3721. (c) Hudnall, T. W.; Gabbai, F. P. *Chem. Commun.* **2008**, 4596. (d) Domaille, D. W.; Zeng, L.; Chang, C. J. *J. Am. Chem. Soc.* **2010**, *132*, 1194. (e) Atilgan, E.; Özdemir, E.; Akkaya, E. U. *Org. Lett.* **2010**, *12*, 4792.

(12) (a) Hattori, S. K.; Urano, Y.; Sunahara, H.; Nagano, T.; Wada, Y.; Tkachenko, N. V.; Lemmetyinen, H.; Fukuzumi, S. *J. Phys. Chem. B* **2005**, *109*, 15368. (b) Erten-Ela, S.; Yilmaz, M. D.; Icli, B.; Dede, Y.; Icli, S.; Akkaya, E. U. *Org. Lett.* **2008**, *10*, 3299. (c) Rousseau, T.; Cravino, A.; Bura, T.; Ulrich, G.; Ziessel, R.; Roncali, J. *Chem. Commun.* **2009**, 1673. (d) Kumaresan, D.; Thummel, R. P.; Bura, T.; Ulrich, G.; Ziessel, R. *Chem.—Eur. J.* **2009**, *15*, 6335. (e) Kolemen, S.; Cakmak, Y.; Erten-Ela, S.; Altay, Y.; Brendel, J.; Thelakkat, M.; Akkaya, E. U. *Org. Lett.* **2010**, *12*, 3812.

(13) (a) Killoran, J.; Allen, L.; Gallagher, J. F.; Gallagher, W. M.; O'Shea, D. F. *Chem. Commun.* **2002**, 1862. (b) Shen, Z.; Röhr, H.; Rurack, K.; Uno, H.; Spieles, M.; Schulz, B.; Reck, G.; Ono, N. *Chem.—Eur. J.* **2004**, *10*, 4853. (c) Goeb, S.; Ziessel, R. *Org. Lett.* **2007**, *9*, 737. (d) Jiao, L.; Yu, C.; Liu, M.; Wu, Y.; Cong, K.; Meng, T.; Wang, Y.; Hao, E. *J. Org. Chem.* **2010**, *75*, 6035.

(14) (a) Baruah, M.; Qin, W.; Vallée, R. A. L.; Beljonne, D.; Rohand, T.; Dehaen, W.; Boens, N. *Org. Lett.* **2005**, *7*, 4377. (b) Yu, Y.-H.; Descalzo, A. B.; Shen, Z.; Röhr, H.; Liu, Q.; Wang, Y.-W.; Spieles, M.; Li, Y.-Z.; Rurack, K.; You, X.-Z. *Chem. Asian J.* **2006**, *1*, 176. (c) Rohand, T.; Baruah, M.; Qin, W.; Boens, N.; Dehaen, W. *Chem. Commun.* **2006**, 266. (d) Deniz, E.; Isbasar, G. C.; Bozdemir, A.; Yildirim, L. T.; Siemiarczuk, A.; Akkaya, E. U. *Org. Lett.* **2008**, *10*, 3401. (e) Atilgan, S.; Ozdemir, T.; Akkaya, E. U. *Org. Lett.* **2008**, *10*, 4065. (f) Buyukcakir, O.; Bozdemir, O. A.; Kolemen, S.; Erbas, S.; Akkaya, E. U. *Org. Lett.* **2009**, *11*, 4644.

(15) (a) Zhao, W.; Carreira, E. M. *Angew. Chem., Int. Ed.* **2005**, *44*, 1677. (b) Zhao, W.; Carreira, E. M. *Chem.—Eur. J.* **2006**, *12*, 7254. (c) McDonnell, S. O.; O'Shea, D. F. *Org. Lett.* **2006**, *8*, 3493.

(16) (a) Jiao, C.; Huang, K.; Wu, J. *Org. Lett.* **2011**, *13*, 632. (b) Jiao, C.; Zhu, L.; Wu, J. *Chem.—Eur. J.* **2011**, *17*, 6610.

(17) Fieser, L. F.; Hartwell, J. L. *J. Am. Chem. Soc.* **1938**, *60*, 2555.

(18) Vellis, P. D.; Mikroyannidis, J. A.; Bagnis, D.; Valentini, L.; Kenny, J. M. *J. App. Polym. Sci.* **2009**, *113*, 1173.

(19) (a) Davis, N. K. S.; Pawlicki, M.; Anderson, H. L. *Org. Lett.* **2008**, *10*, 3945. (b) Davis, N. K. S.; Thompson, A. L.; Anderson, H. L. *Org. Lett.* **2010**, *12*, 2124. (c) Davis, N. K. S.; Thompson, A. L.; Anderson, H. L. *J. Am. Chem. Soc.* **2011**, *133*, 30.

electron-donating 2,4,6-trimethylphenoxy groups were introduced at the 4,5-positions of the anthracene unit in precursor **6**. The bromoanthracene **4**[19c] was treated with *n*-butyllithium followed by addition of anhydrous DMF to give anthracene aldehyde **5** in 63% yield. Similar sequential condensation, oxidative dehydrogenation, and complexation reactions from **5** afforded the anthracene–BODIPY dyad **6** in an overall 67% yield. Compound **6** was treated with excessive $FeCl_3$, yielding the desired ring-fused BODIPY **7a** in 45% yield. Meanwhile, a dimer **7b** was also obtained in 37% yield, which is a product of intermolecular oxidative coupling of **7a** at the β-position of pyrrole ring. Thanks to the presence of bulky 2,4,6-trimethylphenoxy groups, **7a** and **7b** show good solubility in common organic solvents such as toluene, DCM, and THF (Table S1, Supporting Information), and their ^{1}H NMR spectra in solution also display well-split peaks.

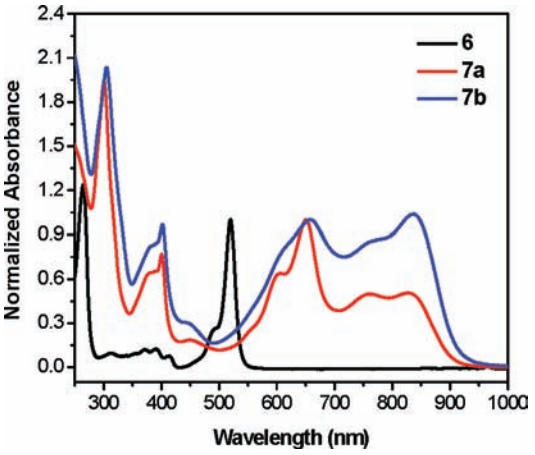

Figure 1. UV–vis–NIR absorption spectra of **6**, **7a**, and **7b** in DCM (1.1×10^{-5} M). The spectra were normalized at 650 nm for **7a** and at 660 nm for **7b**.

The absorption spectrum of precursor **6** in DCM displays the characteristic bands of respective BODIPY and anthracene, while the fused compounds **7a** and **7b** exhibit a significant bathochromic shift (Figure 1). Compound **7a** show absorption maxima at 301 nm (molar extinction coefficient ε = 21800 M^{-1} cm^{-1}) and 401 nm (ε = 8700 M^{-1} cm^{-1}) in the UV–vis range and a broad absorption band located between 500 and 930 nm with maxima at 606 (ε = 7200 M^{-1} cm^{-1}), 650 (ε = 11300 M^{-1} cm^{-1}), 760 (ε = 5600 M^{-1} cm^{-1}), and 826 nm (ε = 5700 M^{-1} cm^{-1}). The dimer **7b** displays a similar absorption spectrum with wavelength slightly red-shifted compared to **7a**, with maxima at 304 (ε = 29000 M^{-1} cm^{-1}), 401 (ε = 13700 M^{-1} cm^{-1}), 613 (ε = 11600 M^{-1} cm^{-1}), 660 (ε = 13800 M^{-1} cm^{-1}), 773 (ε = 12400 M^{-1} cm^{-1}), and 835 nm (ε = 14800 M^{-1} cm^{-1}). The slight red shift can be explained by a large torsion angle between the two BODIPY units in **7b** induced by steric repulsion. Interestingly, the absorption and emission spectra of **7a** and **7b** exhibit obvious solvent dependence (Figures S1 and S2 and Table S1 in the Supporting Information). As the solvent is changed from hexane to toluene, to THF, and to DCM and methanol, the absorption and emission spectra both show a gradual blue shift. This unusual negative solvatochromic effect must be related to the unique H-aggregation of the chromophore in different solvents.

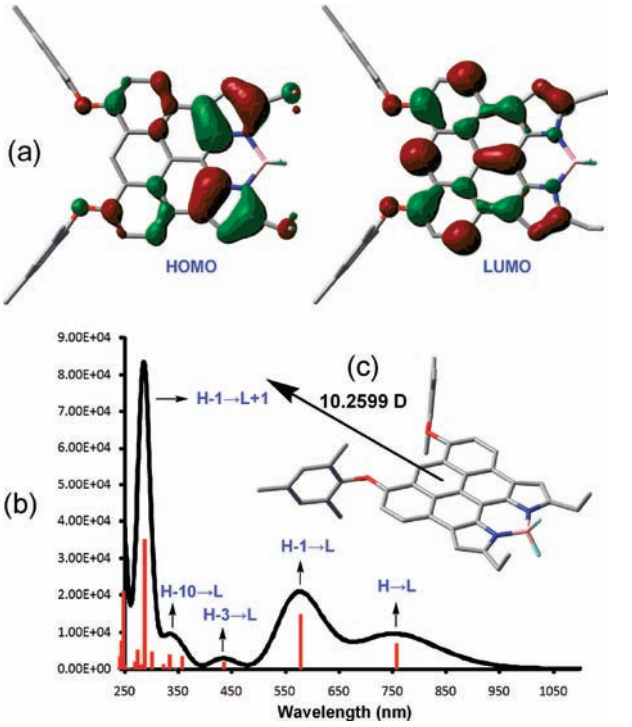

Figure 2. Calculated frontier orbital profiles (a), absorption spectrum (b), and dipole moment (c) of **7a**.

To further understand this solvatochromism phenomenon and to gain better insight into the molecular geometries, molecular orbitals, and UV–vis–NIR absorption spectra, time-dependent density function theory (TDDFT at B3LYP/6-31G*) calculations were performed for **7a**. The optimized geometry, frontier molecular orbital profiles, calculated absorption spectrum, and dipole moment are shown in Figure 2. Compound **7a** has a nearly planar aromatic core, and its HOMO and LUMO are delocalized along the whole π-system, with the HOMO coefficient mainly on the pyrrole rings while the LUMO coefficient mainly on the anthracene unit. Such extended π-conjugation leads to a low optical energy gap of 1.38 eV for **7a**. The calculated electronic absorption spectrum for **7a** discloses a similar spectrum to the experimental data, with absorption maxima at 757 (HOMO→LUMO), 578 (HOMO-1→LUMO), 435 (HOMO-3→LUMO), 333 (HOMO-10→LUMO), and 287 nm (HOMO-1→LUMO+1). Compound **7a** has a large diople moment of 10.2599 D, indicating strong intramolecular charge transfer from the electron-rich anthracene-dipyrromethene unit to the electron-deficient $-BF_2$ unit. As a result, a weak and broad emission band with maximum wavelength at 925 nm was

observed for **7a** and **7b** when detected at the NIR spectral range (Figure S2, Supporting Information). The planar geometry and large dipolement allow antiparallel dimer formation between two planar cores via both $\pi-\pi$ and dipole−dipole interactions. Such a H-type aggregation is more favorable in more polar solvents such as methanol and leads to a blue shift of the absorption spectrum. Similarly, for **7b**, head-to-tail H-aggregate formation is also possible, and thus, it exhibits similar solvatochromic effect to **7a**.

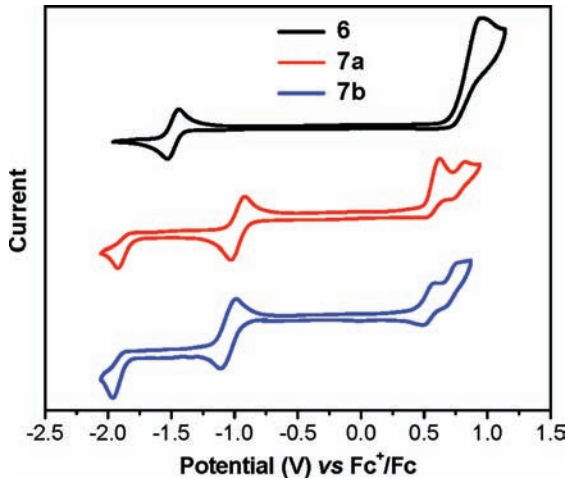

Figure 3. Cyclic voltammograms of **6**, **7a**, and **7b** in DCM with 0.1 M Bu_4NPF_6 as supporting electrolyte, AgCl/Ag as reference electrode, Au disk as working electrode, Pt wire as counter electrode, and scan rate at 50 mV/s. Fc^+/Fc was used as external reference.

The electrochemical behaviors of **6**, **7a**, and **7b** were investigated by cyclic voltammetry in deoxygenated DCM solution containing 0.1 M tetra-*n*-butylammonium hexafluorophosphate as supporting electrolyte. As shown in Figure 3, **7a** displays two reduction waves with half-wave potentials at −0.97 (reversible), −1.88 V (irreversible) and two quasi-reversible oxidation waves with half-wave potentials at 0.57, 0.78 V (vs Fc^+/Fc). A HOMO energy level of −5.30 eV and a LUMO energy level of −3.88 eV were estimated on the basis of the onset potential of the first oxidation and the first reduction wave, respectively. An energy gap of 1.42 eV was obtained from the difference of LUMO energy level and HOMO energy level, which is in agreement with the optical band gap (1.38 eV). Similar results were obtained for **7b**. Compound **7b** shows two reduction waves with half-wave potentials at −1.05 (reversible), −1.92 V (irreversible) and two reversible oxidation waves with half-wave potentials at 0.53, 0.72 V. A HOMO energy level of −5.34 eV and a LUMO energy level of −3.95 eV were calculated by a similar method. An energy gap of 1.39 eV was obtained, which is in agreement with the optical band gap (1.36 eV). The precursor **6** exhibits one irreversible oxidation wave with an onset potential at 0.72 V and one reversible reduction wave with half-wave potential at −1.49 V. The HOMO and LUMO energy levels are calculated to be −5.52 eV and −3.38 eV, respectively, for **6**. Compared with **7a** and **7b**, a larger electrochemical energy gap (2.14 eV) was observed for **6**, which is also consistent with the optical band gap (2.30 eV). Based on these results, we can conclude that ring fusion greatly decreases the LUMO energy level and the energy gap by extending the π-conjugation, leading to a red shift in the absorption spectrum.

The photostability of these compounds in toluene was investigated under white light irradiation (100 W) or UV irradiation (4 W, emission at 254 nm) in air (Figure S3 in the Supporting Information). The absorbance of **7a** and **7b** in air-saturated toluene remained almost unchanged ($<2\%$) after exposure to the irradiation of white light or UV light for 118 h. Under same conditions, the precursor showed about 5% degradation. This observation clearly demonstrates that anthracene-fused BODIPYs **7a** and **7b** have high photostability although an electron-rich anthracene unit is fused. The excellent photostability is of great importance for the practical applications.

In summary, anthracene was successfully fused onto the zigzag edge of a BODIPY core for the first time. The presence of electron-donating 2,4,6-trimethylphenoxy group is necessary for a successful intramolecular cyclization and it also improves the solubility of product. The newly formed compounds **7a** and **7b** showed low band gap and NIR absorption/emission. They also exhibited high photostability, which is crucial for their practical applications. Further structural modifications with the attention to prepare functional anthracene-fused BODIPY dyes for organic field-effect transistors and dye-sensitized solar cells are underway in our laboratories.

Acknowledgment. J.W. acknowledges financial support from the Singapore DSTA DIRP Project (DSTANUS-DIRP/2008/03), an NRF Competitive Research Program (R-143-000-360-281), and an A*Star BMRC grant (no. 10/1/21/19/642). K.-W.H. acknowledges financial support from KAUST.

Supporting Information Available. Experimental details and characterization data of all new compounds and theoretical calculation data. This material is available free of charge via the Internet at http://pubs.acs.org.